Optical Engineering

OpticalEngineering.SPIEDigitalLibrary.org

Zoom into picometer: a picoscale equivalent phase-difference-generating method for testing heterodyne interferometers without ultraprecision stages

Di Chang
Jianing Wang
Pengcheng Hu
Jiubin Tan

SPIE.

Di Chang, Jianing Wang, Pengcheng Hu, Jiubin Tan, "Zoom into picometer: a picoscale equivalent phase-difference-generating method for testing heterodyne interferometers without ultraprecision stages," *Opt. Eng.* **58**(6), 064101 (2019), doi: 10.1117/1.OE.58.6.064101.

Zoom into picometer: a picoscale equivalent phase-difference-generating method for testing heterodyne interferometers without ultraprecision stages

Di Chang,[a,b,†] Jianing Wang,[a,b,†] Pengcheng Hu,[a,b,*] and Jiubin Tan[a,b]
[a]Harbin Institute of Technology, Center of Ultra-precision Optoelectronic Instrument Engineering, Harbin, China
[b]Key Lab of Ultra-precision Intelligent Instrumentation (Harbin Institute of Technology), Ministry of Industry and Information Technology, Harbin, China

Abstract. A simple and low-budget method aiming to generate phase difference equivalent to picoscale-measured displacements of heterodyne interferometers is proposed. By changing the length of an interference arm in an interferometer-like optical configuration, a small phase difference between the two wavelengths is generated for creating the same effect as a picoscale-measured displacement of the heterodyne interferometer. It is derived and experimentally demonstrated that the zoom factor, defined as the ratio of displacements in a heterodyne interferometer and the proposed method leading to the same phase difference, is proportional to the beat frequency and generally in a scale of 10^{-9}. Thus, instead of ultraprecision piezo-stages, only a commercial linear guide rail is equipped in the method, and rigorous vibrating isolation is not necessary. The method has been already used to evaluate signal-processing electronics of a heterodyne grating interferometer. [DOI: 10.1117/1.OE.58.6.064101]

Keywords: heterodyne interferometry; picometer displacements; phase-difference generating.

Paper 190320 received Mar. 7, 2019; accepted for publication May 15, 2019; published online Jun. 5, 2019.

1 Introduction

Interferometers have been deeply investigated and widely equipped during the past decades, resulting in increasing resolutions to meet rising demands. For instance, in the developing semiconductor industry, the metrology of the mask stage and wafer stage is required to attain a measuring resolution in the scale of subnanometers and even picometers.[1,2] Compared to the homodyne ones, heterodyne interferometers are advantageous in optical structure and signal-to-noise ratio (SNR), and are seen as a key approach to high-resolution displacement measurements. Nowadays, more and more researchers around the world are reporting progress in picoscale resolution heterodyne interferometers, including the ones utilized in gravitational wave detection[3] and Joule balance.[4] Meanwhile, as the investigation on the optical nonlinearity existing in heterodyne interferometers goes further, several explanatory theories have been advanced and errors in nanometer and picometers have been revealed.[5–7]

However, it is difficult and expensive to implement a picoscale experiment. Currently, a piezo (PZT)-based microactuator is the prevailing device to generate such a small displacement.[8] But it is hard to find a commercial PZT actuator reaching a resolution of <50 pm. Creating a rigorously vibration-isolation and turbulence-free environment for the PZT actuator and the interferometer is also not an easy task. Thus, some substituting methods are devised to generate equivalent beat-frequency signals. For instance, signal generators are effective devices to simulate reference and measurement signals of heterodyne interferometers. Since its first use for testing electronics of the heterodyne interferometer by Demarest in 1997,[9] the method has been generally accepted and commonly used by engineers, researchers, and staff in metrology institutions.[10] Although the method provides good accuracy and eliminates other sources of the system,[9] a signal generator still could not test the whole signal-detecting and -processing system including photodiodes. Similarly, in the investigations of optical nonlinearity, time-domain analyses such as linear fitting are capable of tackling periodic nonlinear errors in nanometers but inadequate for the smaller ones in picometers because of the amplitude of vibration. Therefore, spectrums are frequently used for distinguishing picoscale periodic nonlinear errors at the cost of losing time-domain information.[11–13]

To test the whole signal-detecting and -processing system of a designing heterodyne grating interferometer, a picoscale equivalent phase-difference-generating method is proposed in this paper. Based on the wavelength difference, a large displacement is zoomed into a small phase difference by the method. Theoretical derivation and experimental tests have proved that a zoom factor is in the order of 10^{-9}, indicating that a phase difference of 1 pm is equivalent to a displacement in several hundreds of millimeters. Thus, the method could be conducted with a commercial linear guide rail instead of expensive PZT actuator in a rigorous environment. In addition, picoscale optical nonlinearity caused by the Zeeman laser in time-domain could also be observed by the method.

2 Principle of the Equivalent Phase-Difference-Generating Method

The equivalent phase-difference-generating method is implemented with an interferometer-like optical configuration, which is depicted in Fig. 1. A dual-frequency laser source (DFLS) emits a laser beam with vertically polarized

*Address all Correspondence to Pengcheng Hu, E-mail: hupc@hit.edu.cn

†These authors contributed equally to this work.

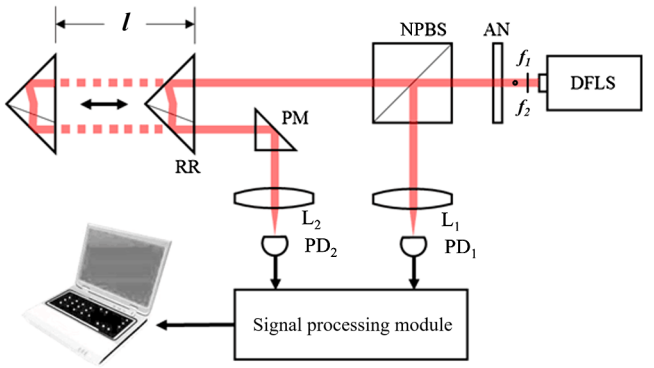

Fig. 1 Schematic representation of the equivalent phase-difference-generating method.

components at different frequencies f_1 and f_2 (assuming $f_1 > f_2$). The beam passes through an analyzer (AN) and becomes an interfering beam. A nonpolarized beam splitter (NPBS) then separates the beam into two parts. The reflected beam enters a lens (L_1) directly and focuses on the photodetector (PD_1), which is acquired as the reference signal. The other part, the transmitted beam straightly enters a moveable corner-cube retroreflector (RR) and is launched back in parallel. A prism mirror (PM) then redirects the beam to another combination of the lens (L_2) and photodetector (PD_2), where the measurement signal with phase difference is obtained. Finally, the reference and measurement signals are sent to the signal-processing module, also called phasemeter in some references, which calculates the equivalent displacement from the phase difference by the same algorithm of a heterodyne interferometer and conveys the results to a host computer for display and recording.

Ignoring the divergence and the Gaussian distribution of intensity in actual laser beams, the two components at different frequencies could be expressed as

$$\mathbf{E}_1(\mathbf{r},t) = \mathbf{A}_1 \cos(\mathbf{k}_1\mathbf{r} - 2\pi f_1 t), \tag{1}$$

$$\mathbf{E}_2(\mathbf{r},t) = \mathbf{A}_2 \cos(\mathbf{k}_2\mathbf{r} - 2\pi f_2 t), \tag{2}$$

where $\mathbf{r}$ is the direction vector, t is the time, $\mathbf{A_1}$ and $\mathbf{A_2}$ are the amplitude vectors and $\mathbf{k_1}$ and $\mathbf{k_2}$ are the wave vectors, whose values are calculated as

$$k_1 = \frac{2\pi}{\lambda_1} = \frac{2\pi n_0 f_1}{c}, \tag{3}$$

$$k_2 = \frac{2\pi}{\lambda_2} = \frac{2\pi n_0 f_2}{c}. \tag{4}$$

Here, λ_1 and λ_2 are the wavelengths corresponding to the two frequencies, n_0 is the refractive index of air, and c is the speed of light in vacuum.

Assuming the optical length of the reference beam (DFLS → NPBS → L_1 → PD_1) is l_0, the alternating intensity i_r that the photodetector PD_1 receives could be expressed as

$$i_r = A_r \cos[(k_1 - k_2)l_0 - 2\pi(f_1 - f_2)t], \tag{5}$$

where A_r is the resultant amplitude. Similarly, assuming l_1 represents the optical length of the measurement beam (DFLS → NPBS → RR → PM → L_2 → PD_2) when the RR is in its initial position, the alternating intensity i_m that the photodetector PD_2 detects could be given as

$$i_m = A_m \cos[(k_1 - k_2)l_1 - 2\pi(f_1 - f_2)t], \tag{6}$$

where A_m is the resultant amplitude. Thus, an initial phase difference is derived from Eqs. (3) to (6),

$$\phi_0 = (k_1 - k_2)(l_1 - l_0) = \frac{2\pi n_0}{c}(f_1 - f_2)(l_1 - l_0). \tag{7}$$

When the RR moves away at a distance of l, the optical length of the measurement beam is increased to $l_1 + 2l$, hence the phase difference is changed to

$$\begin{aligned}\phi_1 &= (k_1 - k_2)(l_1 + 2l - l_0) \\ &= \frac{2\pi n_0}{c}(f_1 - f_2)(l_1 + 2l - l_0).\end{aligned} \tag{8}$$

Therefore, the measured phase difference caused by the movement of RR is expressed as

$$\Delta\phi = \phi_1 - \phi_0 = \frac{2\pi n_0}{c}(f_1 - f_2) \times 2l. \tag{9}$$

Equation (9) describes that the phase difference is proportional to the displacement of the RR, determined by the beat frequency and influenced by the refractive index of air. Further discussions on these influencing factors are introduced in Sec. 4.

Considering a heterodyne interferometer, the relationship between the phase difference $\Delta\phi_0$ and the measured displacement x is given as

$$x = \frac{\Delta\phi_0}{2\pi} \times \frac{\lambda_0}{K} = \frac{\Delta\phi_0 c}{2\pi n_0 f_0 K}, \tag{10}$$

where λ_0 is the wavelength in the reference arm of the heterodyne interferometer, f_0 is the corresponding frequency, and K is the optical fold factor. In a basic heterodyne interferometer, the factor K is equal to 2.

The equivalent displacement x is derived by replacing the phase difference $\Delta\phi_0$ in Eq. (10) with the $\Delta\phi$ in Eq. (9). Actually, the electronics could not tell where the acquired phase differences are from; they just transfer the calculated phase differences to displacements according to an equation similar to Eq. (10). Consequently, a real displacement in the proposed method L is equivalent to a simulated displacement measured by a heterodyne interferometer x according to the following equation:

$$x = \frac{f_1 - f_2}{f_0} \times L. \tag{11}$$

The coefficient in Eq. (11), expressed as $(f_1 - f_2)/f_0$, is defined as the zoom factor. It is obvious that the zoom factor is relative to the beat frequency $f_1 - f_2$ and the laser frequency f_0, which are all determined by the laser source. Generally, the laser frequency is in the order of 10^{14} Hz, whereas the beat frequency is about 10^6 Hz. The zoom

factor, as their ratio, is in the order of 10^{-8} to 10^{-9}, which means that a movement of several millimeters is zoomed into only a couple of picometers by the proposed method. Further, it proves that a common linear guide rail is capable for the method and there is no special requirement on the environment—positioning accuracy and vibration in microns is equivalent to a real displacement in sub-picometer scale, which is much smaller than the resolution of current phasemeters. Thus, there is no need to equip a high-resolution PZT actuator in this method.

3 Experiments

3.1 *Experimental Setup*

The experimental setup is portrayed in Fig. 2. A Zeeman laser (model: HP5517B, Keysight Technology) with a beat frequency ranging from 1.9 to 2.4 MHz is equipped as the laser source. The linear guide rail (model: MTS528, BOCI Company) could support a maximal movement of 1 m with a resolution of ± 50 μm. The testing signal-detecting and -processing system includes two photoreceivers (model: HCA-S-200M-SI, FEMTO), two low-pass filters (model: BLP-5+, MiniCircuits) with a passband from DC to 5 MHz, and a custom-developed phasemeter.[10] In the following experiments, the data are directly conveyed and recorded from the phasemeter to the host computer via a USB interface.

3.2 *Validating the Equivalent Phase-Difference-Generating Method*

The key to validate the proposed method is that the picoscale phase differences are indeed generated with a correct zoom factor. According to Eq. (11), the ratio of measured displacements x/L is used to compare with the zoom factor calculated by the frequencies.

First, by connecting the output of the reference photodetector and a universal frequency counter (model: 53230A, Keysight Technology) with a BNC cable, an average of short-term frequency in 5 min is recorded as 2.200 MHz. Taking the wavelength of He–Ne laser in vacuum as 632.991 nm and the refractive index of air as 1.00027, it is calculated that the theoretical zoom factor is 4.644×10^{-9} at the measured beat frequency. Then, the output signals are reconnected to the phasemeter via the low-pass filters. And the RR is immediately driven to reciprocate from an end of the guide rail to the other, with a maximal displacement of 1000.03 mm. Figure 3 illustrates the data of equivalent displacements calculated by the phasemeter.

In the overview of the reciprocating movements shown in Fig. 3(a), the data in the starting place are marked as sequences A, C, E, and G, and the data in the returning place are marked as B, D, and F. Data distributions of the whole sequences in the starting place are counted and displayed in the left curves of Fig. 3(b), and detailed samples in 1 s for each sequence are shown in the right curves. Similarly, Fig. 3(c) illustrates the data distributions and the detailed samples of sequences B, D, and F. The actually measured data indicate that the equivalent displacement is 4.664 nm, and further reveal a zoom factor of 4.664×10^{-9}. The result is acceptable and the method is validated. The deviation of the measured and derived zoom factors is considered to be mainly caused by the optical nonlinearity, which will be described in the following Sec. 4.

3.3 *Comparison of the Phase-Difference-Generating Method and a Signal Generator*

The equivalent phase-difference-generating method could be used for testing the static performance of heterodyne interferometers by providing signals with noises from real laser sources and photodetectors. A comparison between the proposed method and a signal generator (Tektronic, model: AFG3252) is conducted. Before the comparison, the frequency spectrums of the signals from the participants being adjusted to similar amplitudes are acquired and are depicted in Fig. 4.

The phases of the signals from the used generator could be set with a minimum step of 0.01 deg, whose results are portrayed in Fig. 5(a). It is indicated that the steps at the phase difference of 0.01 deg and 0.03 deg are unstable. Then, the phase step of 0.02 deg is equivalent to a displacement of 17.6 pm. Similarly, the step movement of the linear guide rail can also create incremental phase differences. The experimental data in Fig. 5(b) represent the steps of RR in 4 mm, which is equivalent to 18.58 pm.

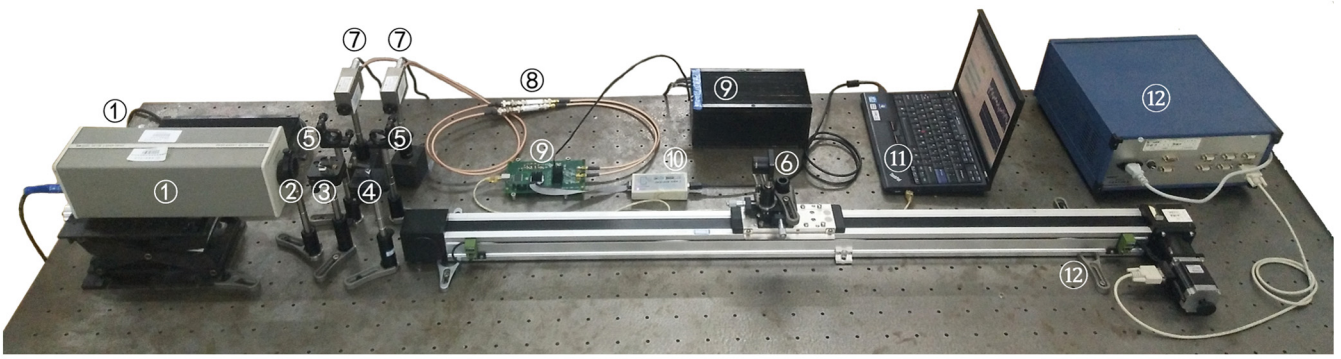

① Dual-frequency laser with DC source;
② Analyzer;
③ Non-polarized beam splitter;
④ Prism mirror;
⑤ Lenses;
⑥ Corner-cube retro-reflector;
⑦ Photo-receivers;
⑧ Low pass filters;
⑨ Phasemeter with DC source;
⑩ USB blaster for FPGA;
⑪ Host computer;
⑫ Linear guide rail with control box.

Fig. 2 Experimental setup.

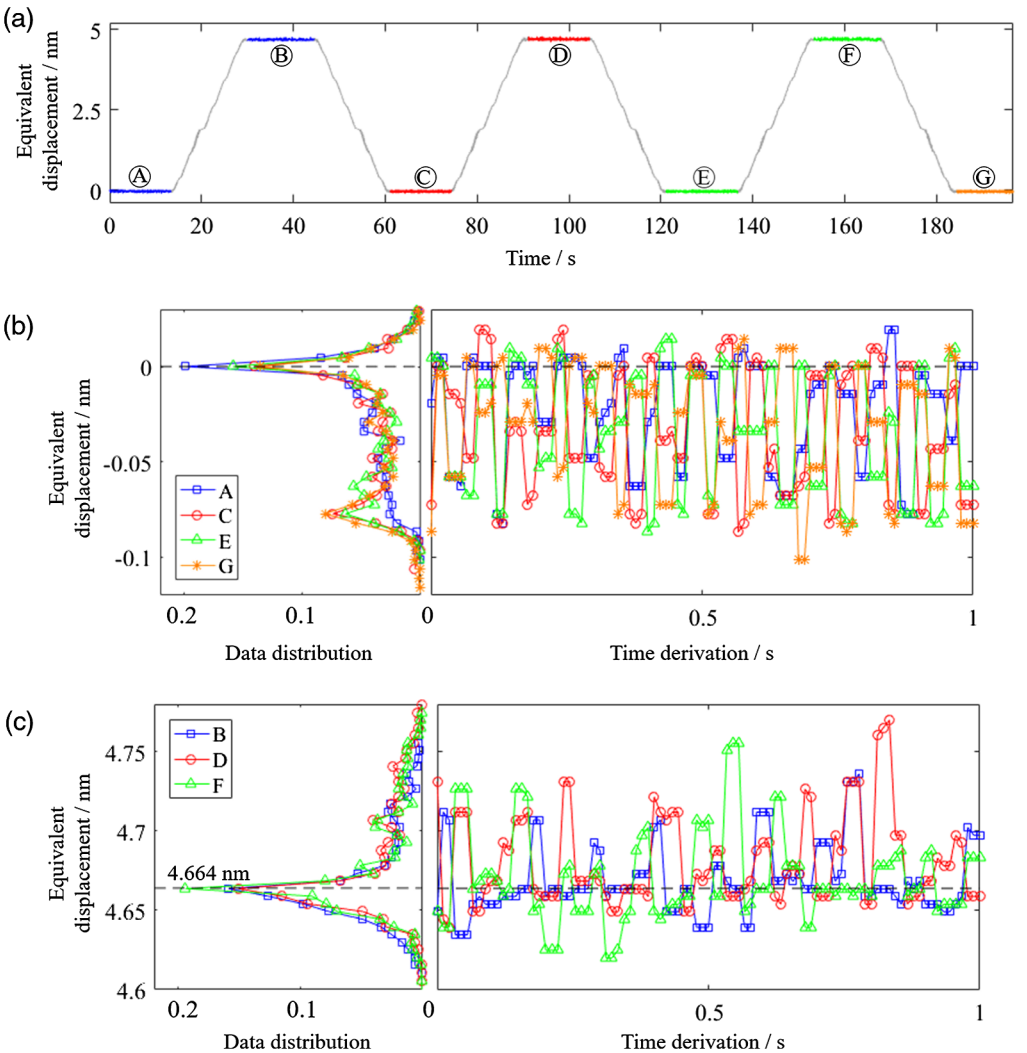

Fig. 3 Measurement results of validating the phase-difference-generating method. (a) An overview of the reciprocating movements. (b) Data distributions of the whole sequences of (a), (c), (e), and (g), with a detailed part in 1 s for each. (c) Data distributions of the whole sequences of (b), (d), and (f), with a detailed part in 1 s for each.

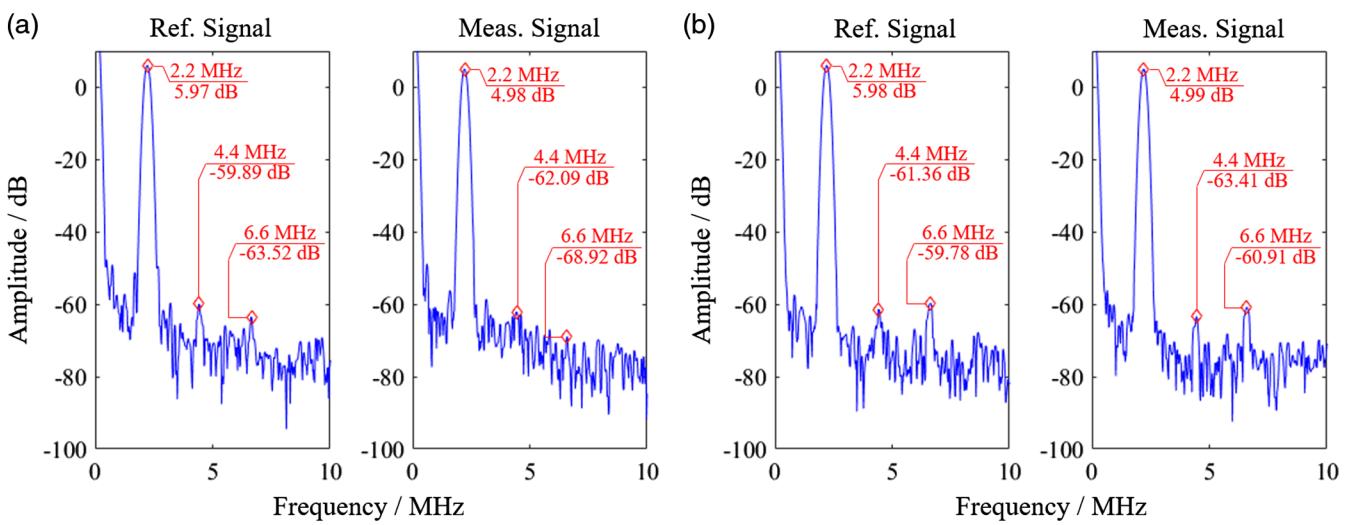

Fig. 4 Frequency spectrums for comparing the proposed equivalent phase-difference-generating method and a signal generator. (a) Spectrums of the signals from a generator and (b) spectrums of the signals from a generator acquired by photodetectors.

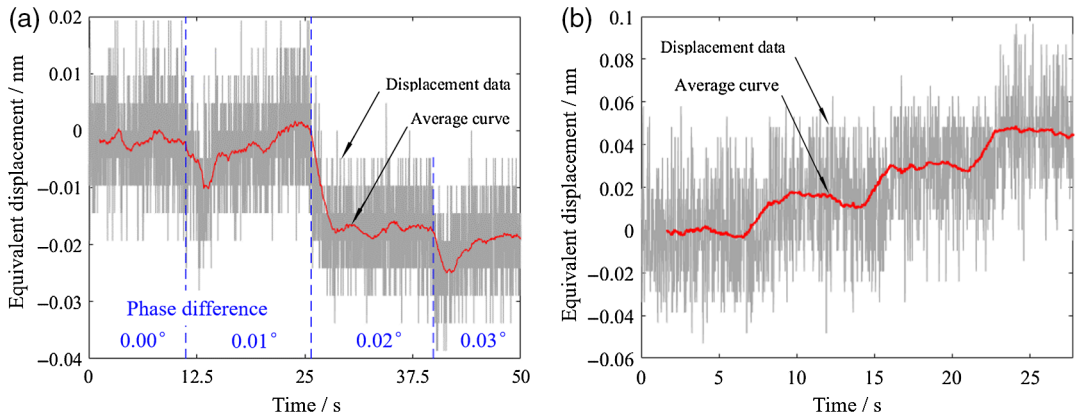

Fig. 5 Equivalent displacement results in steps. (a) The 0.01-deg phase step from the signal generator and (b) the 4-mm displacement step from the guide rail.

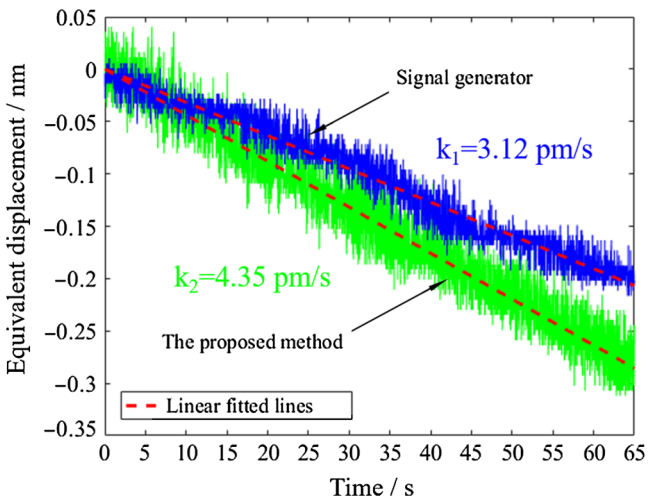

Fig. 6 The equivalent displacement curves and the fitting line at the minimal speed of the proposed method and the signal generator.

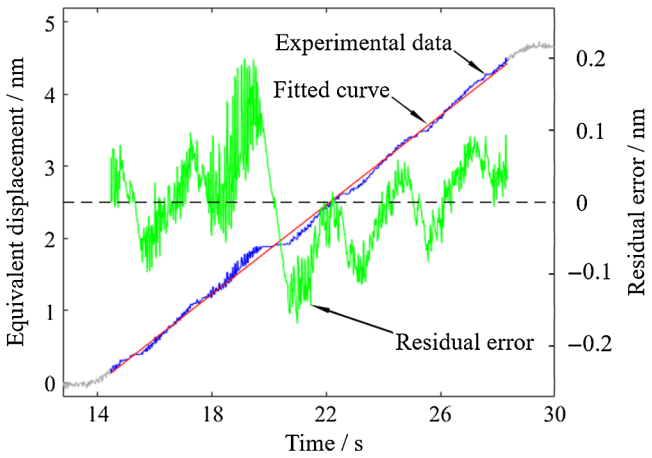

Fig. 7 Optical nonlinear errors in the time domain and the residual error of linear fitting.

It can be concluded that the signal generator provides a displacement with fewer noises; its signals are more ideal than the real signals acquired by photodetectors. And the proposed equivalent phase-difference-generating method has the potential for smaller steps. In the experimental setup, the minimum step of the equivalent displacement is determined by the product of the resolution of the guide rail and the zoom factor, which is calculated as ± 0.2322 pm, which is enough for a picoscale heterodyne interferometer.

Then, the minimum frequency difference of the used signal generator is 10 μHz. The equivalent velocity under such an optical Doppler frequency is theoretically calculated as 3.16 pm/s. The corresponding displacement is shown as the blue curve in Fig. 6, whose fitting line has a slope of 3.12 pm/s. The deviation is attributed to the nonlinearity. Likewise, the lowest speed of the equipped linear guide rail is about 0.94 mm/s, which is zoomed into 4.35 pm/s by the proposed method. Figure 6 shows that the green line and its fitting slope are consistent with the derivation.

Figure 6 also displays that the optical nonlinearity of the blue line is more obvious than the green line, which could explain that the redundant peaks at 4.4 and 6.6 MHz in Fig. 4(b) are lower than those in Fig. 4(a), and the nonlinearity they caused is drowned in noises.

Similarly, the data acquired during the movement in Fig. 3(a) are expected to be a straight line with certain fluctuations caused by noises, however. Contrarily, a large platform and several small ones in certain places could be easily observed in the reciprocating movement. It is proved that the locations of the platforms are irrelevant to the guide rail but related to the laser by changing the relative distance between them, which means that the platforms are caused by the laser beam, rather than the guide rail, phasemeter circuits, and algorithm. Thus, the nonlinearity is attributed to the heterodyne laser source. As Fig. 7 shows, the data extracted from Fig. 3(a) are shown in the blue curve and fitted by a linear function. The residual error in the green curve indicates that the observed nonlinear errors are about 0.3 nm. Therefore, the method could also be used for observing optical nonlinearity caused by the laser source.

In summary, the comparison of the proposed equivalent phase-difference-generating method and the commonly used signal generator are concluded in the following table (Table 1). To achieve a complete comparison, a heterodyne interferometer with PZT stage is also listed. By providing real optoelectronic signals, the proposed method could be used for testing the static feature of phasemeters, especially those for picoscale measurement. In addition, optical

Table 1 Comparison of the equivalent phase-difference-generating method, the signal generator, and a heterodyne interferometer with PZT stage.

	Equivalent phase-difference-generating method	Signal generator	Heterodyne interferometer with PZT stage
Devices under test	Phasemeter, laser source, and photodetectors.	Phasemeter only.	The whole interferometer.
Noise and nonlinearity	Noise and nonlinearity caused by laser and photodetectors are included. Interfering signals are closer to the real case.	The signals are more ideal with fewer fluctuations.	Real noise and nonlinearity caused by the laser, prisms, and the photodetectors.
Stepping of phase	Continuous. Determined by the movement resolution of the guide rail.	Discrete. Quantized by the minimal increment of the phase.	Continuous. Determined by the resolution of the PZT stage.
Range	Limited by the guide rail. Typically within several nanometers.	Infinite. Unless the registers are overflowed.	Limited by the stage. Usually in several tens to hundreds of microns.
Simulated moving speed	Zoomed by the factor. Restricted in the scale of pm/s.	Ranges from pm/s to m/s.	Usually no larger than mm/s.
Resistance to environmental disturbance	The influence of vibration and air turbulence is negligible.	Free of vibration and air turbulence.	Influenced by the surrounding vibration and air turbulence.

nonlinearity caused by heterodyne laser could be separated and observed. Combination of these two methods will provide more detailed information about the tested heterodyne interferometer for design, evaluation, and investigation.

4 Discussions

It has been proved that the experimental zoom factor is consistent with the theoretical value with an acceptable error. However, in the experiments above and other possible applications, the results are also influenced by several errors such as the alignment error, beat frequency fluctuation, environmental disturbance, and optical nonlinearity. These errors could be classified into two types: geometrical errors and optical errors.

4.1 *Geometrical Errors*

The geometrical errors, acting on the optical length L in the Eq. (11), are caused by the Abbe error and vibration. Since the laser source and the linear guide rail are spatially assembled, it is impossible to make them perfectly parallel with each other. As shown in the coordinates in Fig. 8, the misalignment angles β and γ lead to a two-dimensional alignment error. In addition, considering the vibration $L_v(t)$, the actual optical path L_{actual} is expressed as

$$L_{\text{actual}} = [L_{\text{rail}} + L_v(t)]\sqrt{1 + \tan^2\beta + \tan^2\gamma}, \tag{12}$$

where L_{rail} represents the displacement of the guide rail including the positioning error. As mentioned above, the positioning resolution of the utilized linear guide rail is $\pm 50\ \mu$m.

Measured by an interferometer, the maximum vibration of the retroreflector $L_v(t)$ is about $\pm 1\ \mu$m. And the misalignment angles could be estimated by observing the position changes of the laser spot on the surface of the RR when driving the linear guide rail, whose values are about 10^{-3} rad. Substitute the angles β and γ in Eq. (12) with the values 10^{-3} rad, the factor of Abbe error is approximately equal to 1. Thus, the influence of Abbe error could be ignored.

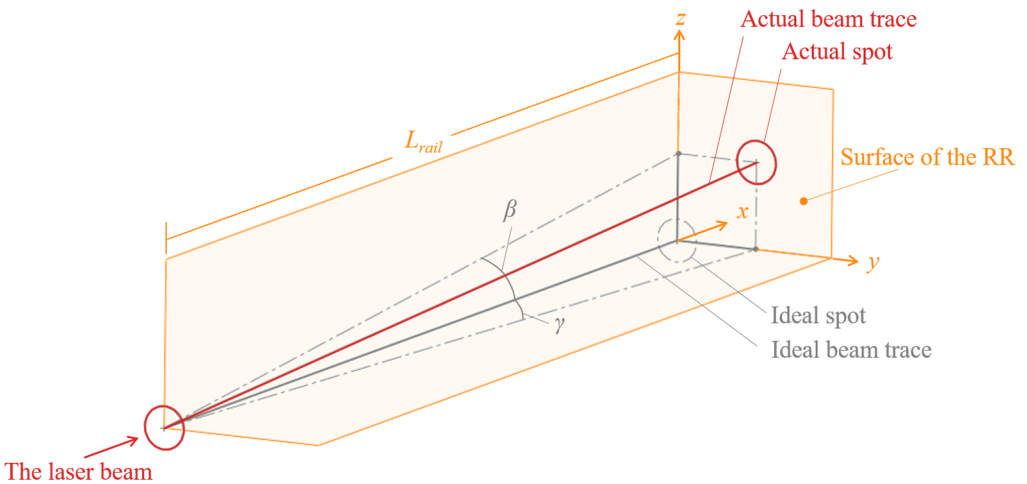

Fig. 8 Schematic representation of the two-dimensional alignment error.

Considering the optical fold factor and the quantification by the 16-bit ADCs, the theoretical resolution of the phasemeter at a measuring wavelength of 632.8 nm is about 4.8 pm. It is indicated that only a geometrical error >1.034 mm could affect the least significant bit (LSB). Thus, the discussed geometrical error in several tens of microns is far from the LSB. It also proves that the proposed method could work in an ordinary lab (without extra vibration isolation).

4.2 *Optical Errors*

The optical errors of the proposed method are subdivided into beat-frequency fluctuation, environmental influence, and optical nonlinearity.

According to the Edlén equation, the index of air refraction is varied with temperature, humidity, and barometric pressure. It will further affect the laser wavelength. Considering the common optical path configuration in Fig. 1, two parts of the laser in different frequencies share the same local environmental parameters. It means that the ideal air refraction n_0 in Eq. (9) will be replaced by a n_{edlen} with actual parameters. Therefore, the zoom factor derived from the modified Eq. (9) and the Eq. (10) is expressed as

$$\text{Zoomfactor} = \frac{x}{L} = \frac{n_{\text{edlen}}}{n_0} \cdot \frac{f_1 - f_2}{f_0}. \tag{13}$$

The changes in environmental parameters are acquired by sensors. During the measuring period, the maximal fluctuation of the temperature, humidity, and the barometric pressure are 0.24°C, 2.3%RH, and 0.14 kPa, respectively. The real-time monitored air refraction n_{edlen} is no less than 1.000271. Thus, the amplification factor n_{edlen}/n_0 is approximate to 1, indicating that the environmental turbulence is negligible.

As a key parameter in the proposed method, the fluctuation of the beat frequency $\Delta f(t)$ will directly change the zoom factor in a linear way. Here, the zoom factor could be expressed as

$$\text{ZoomFactor} = \frac{x}{L} = \frac{f_1 - f_2}{f_0} + \frac{\Delta f(t)}{f_0}. \tag{14}$$

Figure 9 displays the beat-frequency data acquired by the frequency counter. The peak-to-peak fluctuation is ±3.2 kHz, accounting for ±0.14% of the average beat frequency. It means that the zoom factor will suffer an undulation of $\pm 0.006 \times 10^{-9}$.

In Sec. 3.3, the optical nonlinearity in curves are observed and analyzed briefly. Generally, the displacement errors caused by optical nonlinearity are relevant to the amplitude of the redundant frequency peaks, such as the double and triple of the base signal. It could be as large as several hundreds of picometers. If the beginning and the end are just influenced by the nonlinearity, the measured equivalent displacement may be far from correct. Therefore, when the proposed method is used for evaluating signal-processing electronics, the platform should be avoided by changing the relative position between the laser and the guide rail.

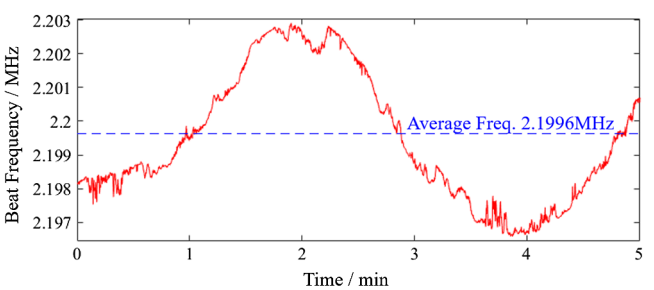

Fig. 9 Fluctuation of the beat frequency acquired by the uniform frequency counter.

5 Conclusions

In this paper, a picoscale equivalent phase-difference-generating method is proposed for evaluating the signal-processing electronics of a heterodyne interferometer. Based on an interferometer-like optical configuration, the proposed method could work with a commercial linear guide rail on an optical platform without extra vibration isolation. Theoretical derivation and experimental verification proved that the generated equivalent phase difference is proportional to the displacement of the linear guide rail, with a zoom factor in the scale of 10^{-9}. The method has the potential to simulate displacements in picometer and even smaller scale measured by heterodyne interferometers, especially in an actual situation with noises from photodiode and amplifier circuits. Future improvements of the method could be in the following aspects: (a) enlarging the moving range of the linear guide for a wider horizon of optical nonlinear errors in time domain, (b) equipping a PZT stage on a vibration platform for simulation a displacement in femtoscale for next-generation heterodyne interferometers, and (c) splitting the beam into spatially separated interferometer for further investigating the nonlinear errors.

Acknowledgments

The authors acknowledge gratefully the support of the National Natural Science Foundation of China (Project code: 51675138) and the National Science and Technology Major Project (Project code: 2017ZX02101006-005). The authors declare no conflict of interest.

References

1. M. Asano et al., "Required metrology and inspection for nanoimprint lithography," *Proc. SPIE* **10145**, 101450J (2017).
2. H. Lin et al., "A 3D translation stage calibrated with Michelson interferometers," *Proc. SPIE* **9958**, 99581A (2016).
3. H. Liu et al., "The development of phasemeter for Taiji space gravitational wave detection," *Microgravity Sci. Tec.* **30**(6), 775–781 (2018).
4. Y. Bai et al., "A six-axis heterodyne interferometer system for the Joule Balance," *IEEE Trans. Instrum. Meas.* **66**(6), 1579–1585 (2017).
5. P. Hu et al., "Toward a nonlinearity model for a heterodyne interferometer: not based on double-frequency mixing," *Opt. Express* **23**(20), 25935–25941 (2015).
6. H. Chen et al., "Synthetic model of nonlinearity errors in laser heterodyne interferometry," *Appl. Opt.* **57**(14), 3890–3901 (2018).
7. H. Fu et al., "Nonlinear errors resulting from ghost reflection and its coupling with optical mixing in heterodyne laser interferometers," *Sensors* **18**, 758 (2018).
8. Physik Instrumente (PI) GmbH & Co. KG, "LISA linear actuator and stage P-753," (2018) https://www.physikinstrumente.com/en/products/nanopositioning-piezo-flexure-stages/linear-piezo-flexure-stages/p-753-lisa-linear-actuator-stage-200900/#downloads (accessed 28 January 2019).
9. F. C. Demarest, "High-resolution, high-speed, low data age uncertainty, heterodyne displacement measuring interferometer electronics," *Meas. Sci. Technol.* **9**, 1024–1030 (1998).
10. H. Fu et al., "Measurement method for nonlinearity in heterodyne laser interferometers based on double-channel quadrature demodulation," *Sensors* **18**, 2768 (2018).

11. V. G. Badami and S. R. Patterson, "A frequency domain method for the measurement of nonlinearity in heterodyne interferometry," *Precis. Eng.* **24**(1), 41–49 (2000).
12. X. Xing et al., "Spatially separated heterodyne grating interferometer for eliminating periodic nonlinear errors," *Opt. Express* **25**(25), 31384–31393 (2017).
13. S. Yokoyama et al., "A heterodyne interferometer constructed in an integrated optics and its metrological evaluation of a picometre-order periodic error," *Precis. Eng.* **54**, 206–211 (2018).

Di Chang is a doctoral candidate at the Harbin Institute of Technology (HIT), China. He received his BS in engineering from HIT and joined the bachelor-straight-to-PhD program in 2016. His current research interests include the optical structure, photodetector, phasemeter, and signal-processing algorithm in the heterodyne grating interferometer.

Jianing Wang is a postgraduate student at the HIT, China. He received his BS degree in engineering from HIT and joined the successive master-doctor program in 2018. Currently, he is working on research about grating interferometry for displacement measurement.

Pengcheng Hu received his BS, MS, and PhD degrees in instrument science and technology from the HIT, Harbin, China, in 2001, 2003, and 2008, respectively. In 2008, he joined HIT as a lecturer; he has been a professor since 2015. From 2009 to 2010, he was a visiting scholar at Physikalisch-Technische Bundesanstalt, Braunschweig, Germany. His current research interests include high-precision sensors and instruments.

Jiubin Tan received his PhD in instrument science and technology from the HIT, Harbin, China, in 1991. He joined HIT in 1982, where he is currently a professor. His current research interests include ultraprecision optoelectronic instrument engineering, photoelectric information detection and processing technology, nanomeasurement technique, and instrument engineering.